Electrode Potential-Dependent Anion Chemisorption and Surface Bond Polarization As Assessed by Density Functional Theory

Sally A. Wasileski* and Michael J. Weaver

Department of Chemistry, Purdue University, West Lafayette, Indiana 47907-1393

Received: January 17, 2002

The electrostatic field-dependent energetics of low-coverage halogen chemisorption on (111) planes of platinum, gold, silver, and mercury are examined by means of Density Functional Theory (DFT) using finite metal clusters, with the primary aim of describing such behavior in relation to potential-dependent halide adsorption at electrochemical interfaces. The general relationship between the field-dependent and electrode potential-dependent adsorption energies of such neutral and ionic species is clarified in terms of the static surface−adsorbate dipole moment, μ_S. The sensitivity of the DFT-based μ_S values to the metal cluster size and geometry is examined. Better agreement with experimental low-coverage μ_S estimates, obtained from work function−coverage data at metal−vacuum interfaces, requires metal clusters extending to at least second-nearest-neighbor atoms in the surface plane. The μ_S DFT values for metal−halogen bonding are also compared with experimental estimates extracted from electrochemical thermodynamic data. The markedly ($\geq$2−3-fold) larger $-\mu_S$ values for the latter reflect the role of inner-layer solvation in inducing greater surface bond polarization. Comparable increases in $-\mu_S$ values calculated from DFT are also obtained by including interfacial solvent molecules modeled as dielectric spheres. The sensitivity of the dipole moment to the interfacial field as deduced by DFT is also noted in relation to observed electrochemical behavior.

Introduction

Given the widespread occurrence of anion chemisorption, especially halides and pseudohalides, in electrochemical systems, understanding the chemical bonding factors involved is of substantial practical as well as fundamental interest. Traditionally, anion adsorption was described purely in terms of electrostatic surface interactions.[1] This view was encouraged by thermodynamic double-layer analyses based on the so-called "ideally polarized electrode" formalism, applied largely to mercury−aqueous interfaces.[1] In recent years, however, the importance of covalent as well as ionic interactions in metal electrode−anion binding has increasingly been recognized.[2−5] This is encouraged by the much greater emphasis now placed on solid metals, especially platinum-group and coinage-metal surfaces, facilitated by the emergence of reliable methods for the preparation and in-situ characterization of oriented monocrystalline electrodes. In turn, the availability of such in-situ spectroscopic and spatial microscopic information on electrode−adsorbate bonding, especially on Pt-group metals, has triggered increasing intercomparison with analogous well-studied metal−ultrahigh vacuum (UHV) interfaces, thereby forging multifaceted new links between electrochemical and UHV-based surface science.[6]

Our understanding of metal−chemisorbate bonding has been heightened notably in recent years by advances made in computational quantum chemistry, especially by means of Density Functional Theory (DFT) utilizing either finite metal clusters or periodic slabs as models.[7] Aside from yielding binding-site energetics, adsorbate vibrational frequencies and even adlayer spatial structures that are often in reasonable accordance with measured quantities, such approaches can provide insight into adsorbate bonding properties that are inaccessible to experiment. This virtue of DFT in providing a more complete quantum-chemical bonding picture is particularly germane to electrochemical systems, given that the breadth of experimental information on metal electrode−chemisorbate interactions remains decidedly narrower than that attainable at metal−UHV interfaces.

Of particular electrochemical interest is the manner and extent to which the metal−adsorbate bonding interactions depend on the applied electrode potential or the interfacial field. The applied surface potential ϕ, and hence electrostatic field F, across electrochemical interfaces can be varied markedly (typically by $\Delta\phi \sim 1$ to 2 V; $\Delta F \sim 0.3$ to 0.6 V Å^{-1}), yielding substantial alterations in surface bonding and electronic structure. Several groups have undertaken ab initio[8,9] and latterly DFT calculations[10−14] using finite metal clusters where the effects of the adjustable surface potential are mimicked by applying a variable external electrostatic field across the cluster−adsorbate assembly. Our own activities on this topic are motivated centrally by a longstanding interest in utilizing in-situ vibrational methods, specifically surface-enhanced Raman scattering (SERS) and infrared reflection-absorption spectroscopy (IRAS), to explore electrode−adsorbate bonding.[15] The particular value of the field-dependent cluster DFT calculations in this regard lies in their capability of relating observed electrode potential-dependent vibrational frequencies to other properties of metal electrode−adsorbate potential-energy surfaces, including equilibrium bond distances and binding energies, along with specific orbital and steric interaction components, which are usually inaccessible to experiment. In addition to the diatomic chemisorbates CO and NO,[13,14b,c] we have recently examined simple monatomic adsorbates, especially the halogens, oxygen, and sulfur,[14] thereby focusing attention on the field-dependent metal−adsorbate bond itself.

* Corresponding author: email: swasile2@purdue.edu.

10.1021/jp020150r CCC: $22.00
Published on Web 04/17/2002

Another interesting aspect of such quantum-chemical calculations stems from the insight so obtained into the nature of the field-dependent binding energetics, more specifically the extent of surface bond polarization. This issue is examined here, with particular reference to the role of metal−adsorbate bond polarization (as expressed as a surface dipole moment) in determining the *field*-dependent binding energies of formally uncharged adsorbates, as extracted from DFT-based calculations (and also of relevance to metal−UHV systems), in relation to the *potential*-dependent adsorption of ionic solute species at electrochemical interfaces. Reported are DFT results for hollow-site adsorption of halogens on platinum, gold, silver, and mercury (111) surfaces in the absence and presence of a solvent dielectric. The last three metals were chosen in view of the availability of quantitative electrochemical thermodynamic data for halide adsorption. The DFT estimates of surface−halogen dipole moments are also compared with corresponding electrochemical data in order to elucidate how double-layer solvation may influence the extent of surface bond polarization.

Computational Methods

The finite-cluster DFT calculations reported here largely follow those described in refs 12−14. While a number of cluster geometries were examined (vide infra), the majority of calculations utilized an isolated adsorbate bound to a 13- or 33-atom C_{3v} symmetry (111) metal cluster, arranged in two layers containing six and seven atoms for the former cluster and 21 and 12 atoms for the latter. The metal interatomic distance was fixed at the experimental bulk-phase value: 2.775 Å (Pt), 2.889 Å (Au), 2.885 Å (Ag), and 3.01 Å (Hg). [While there is some uncertainly in the effective interatomic distance (and interfacial structure) for liquid mercury, the DFT results were not affected significantly by increasing the quoted value by a few percent.] Adsorbates were bound in threefold-hollow binding geometries (hcp for the 13-atom cluster and fcc for the 33-atom cluster).

All calculations utilized the Amsterdam Density Functional (ADF) package.[16] Slater-type functions were used to represent the atomic orbitals. To enhance computational efficiency, the innermost atomic shells of all atoms (up to and including the following orbitals: Ag 4p, Pt 5p, Au 5p, Hg 5p, Cl 2p, Br 3p, I 4p) were kept frozen, as these core electrons do not contribute significantly to the chemical bonding. The Ag, Au, Pt, and Hg basis sets were of double-ζ quality; in addition, the Cl and Br basis sets were augmented by polarization functions. The Kohn−Sham one-electron equations were solved in the DFT-GGA approximation. The Vosko−Wilk−Nusair form of the local density approximation[17a,b] was used in combination with the BP86 functional for the generalized gradient approximation.[17c] Relativistic effects within the cores were accounted for self-consistently by first-order perturbation theory. All cluster calculations were carried out in the spin-restricted mode, while isolated atom calculations were undertaken in the spin-unrestricted mode.

Hirshfeld charges[18] and static dipole moments were obtained from the standard ADF output. The static dipole moment μ_S (and binding energy) for the M−X bond were determined by subtracting the dipole moment (and energy) calculated for the bare cluster (and also the isolated adsorbate) from that for the ligated cluster. The DFT calculations for solvated clusters employed the ADF "Conductor-like Screening Model" (COSMO),[16b] which embeds the cluster in a cavity surrounded by a continuous dielectric (vide infra). The cavity geometry was determined by packing an infinite number of solvent dielectric spheres (taken to be 2.8 Å diameter, appropriate for water) around the cluster−adsorbate assembly. The closest approach of the dielectric sphere was determined by taking the metal "van der Waals" radii to be 0.7 Å larger than the metallic values and the Cl, Br, and I radii as 1.8, 1.95, and 2.1 Å, respectively. (The resulting μ_S values, determined by using the adsorbate-free solvated cluster as a reference state, were insensitive to these radii choices, at least for variations within 0.1−0.2 Å.) This approach mimics roughly the anticipated closest approach of solvent dielectric spheres to the metal atomic plane.

Results and Discussion

General Relation between Field-Dependent and Electrode Potential-Dependent Ionic Chemisorption. As a starting point, it is necessary to clarify the general relationship between the field-dependent metal−adsorbate binding as obtained from DFT with the potential-dependent energetics of ionic adsorption at metal−solution interfaces. The metal-cluster DFT calculations undertaken here involve binding an initially *uncharged* adsorbate (e.g., Cl, O, CO, etc.) at a suitable site on the metal surface. We select a given binding-site geometry (here threefold hollow) and vary the surface−adsorbate distance to yield the minimum energy (i.e., the equilibrium) configuration. The metal−adsorbate binding energy, E_b, is obtained from the energy decrease upon forming this configuration from the separated cluster and adsorbate. To mimic alterations in electrode potential, the metal cluster (but not the uncoordinated adsorbate) is placed in a variable uniform electrostatic field, F, oriented normal to the metal surface.

The dependence of the binding energy on the external field is given by[14a−c,19]

$$-\mu_S = (\mathrm{d}E_b/\mathrm{d}F) \tag{1}$$

where μ_S is the metal−adsorbate static dipole moment, evaluated as the difference in the metal cluster dipole parallel to the field in the presence and absence of the adsorbate. Equation 1 is generally valid at any field if higher-order multipole terms can be neglected, which is the case to a very good approximation for the conditions of interest here,[14b] in the presence as well as absence of interfacial solvent. The obvious importance of eq 1 is that it describes the sensitivity of the metal−adsorbate bond energy to the interfacial field (as evaluated by DFT with electrochemical systems in mind) to the extent of surface bond polarization as described formally by the dipole moment. As utilized below, experimental estimates of μ_S at metal−UHV interfaces (usually for $F = 0$) can be obtained from the dependence of the surface work function on the adsorbate coverage.[20]

At electrochemical interfaces, however, the electrode potential rather than the field constitutes the experimentally accessible electric variable. Nonetheless, if we consider the potential drop $\Delta\phi$ to be roughly linear across the inner part of the double layer, of thickness x_2, then

$$(\mathrm{d}E_b/\mathrm{d}F) = x_2(\mathrm{d}E_b/\mathrm{d}\phi) \tag{2}$$

A closely related, and measurable, quantity is the electrode-potential dependence of the free energy of adsorption ($\mathrm{d}\Delta G^\circ/e\,\mathrm{d}\phi$) where e is the electronic charge. In particular, the so-called "electrosorption valency" (or "formal charge-transfer coefficient"), γ, often considered in electrochemical thermodynamic analyses, is related to this quantity by[21]

$$\gamma = (\mathrm{d}\Delta G^\circ/e\,\mathrm{d}\phi) = -(\partial\sigma_m/e\partial n)_\phi \tag{3}$$

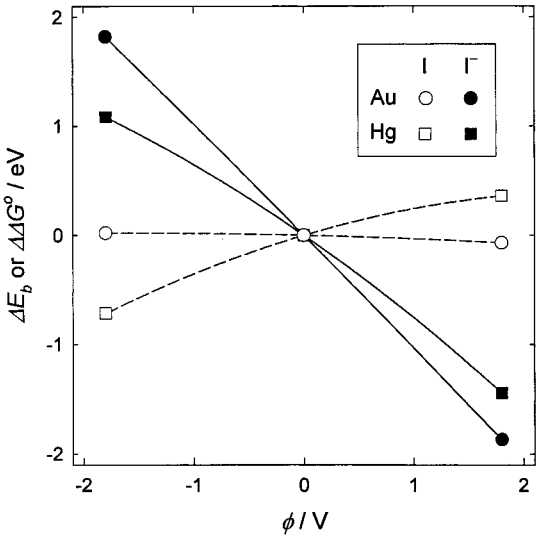

Figure 1. Illustration of the form of surface potential-dependent binding energy of halogen, E_b, as obtained by DFT for unsolvated Au_{13}−I and Hg_{13}−I systems (filled circles and squares, respectively), in comparison with the corresponding potential-dependent adsorption energy of halide, ΔG^o, as extracted by using eq 4 (open circles and squares, respectively).

where σ_m is the excess electronic charge density on the metal, and n is the adsorbate surface concentration (expressed as atoms or molecules cm^{-2}). For charged adsorbates, γ can be considered to reflect the extent to which this charge moves through the double-layer potential drop toward the metal upon adsorption.[21] For example, in the extreme case where essentially complete charge transfer to the metal occurs upon adsorption, then $\gamma = z$, where z is the charge number of the adsorbing ion in solution.

Provided that the potential dependence of the adsorption entropy can be neglected, we can generally relate (dE_b/dF) and $(d\Delta G°/e\ d\phi)$ for a given system by[14a,c]

$$(dE_b/e\ d\phi) = (d\Delta G°/e\ d\phi) - z \tag{4}$$

Equation 4 accounts for the important difference in reference state for E_b and $\Delta G°$ in that these quantities refer to adsorption of *uncharged* and *charged* bulk-phase species, respectively. [Commonly, then, the two differential coefficients in eq 4 will have *opposite signs*.] For example, adsorption of electronegative atoms such as chlorine will yield stronger binding, i.e., larger $-E_b$ values, toward more *negative* surface potentials/fields, whereas the same process involving *chloride* yields larger $-\Delta G^o$ values toward more *positive* surface potentials, even though the final adsorbed state is identical. This difference, and hence the form of eq 4, simply reflects the surface potential-dependent energy of moving a charge ze completely across the interface, required in order to transform between the charged and uncharged bulk-phase reference states. The relation between E_b and ΔG^o at zero external field ($F = 0$) for a monocharged anion, X^-, can be written as[4a]

$$E_b(X) = \Delta G^o(X^-) + EA(X) + \Delta G_{solv} - \Phi_m \tag{4a}$$

where EA(X) is the (negative-sign) electron affinity of the halogen, ΔG_{solv} is the ionic solvation energy, and Φ_m is the metal work function of the uncharged ($F = 0$) interface. Representative plots of E_b and ΔG^o versus the surface potential ϕ, normalized for convenience to their values at $F = 0$ (and $\phi = 0$), are shown for Au(111)−I and Hg(111)−I in Figure 1. The $\Delta E_b-\phi$ curves (filled symbols, solid lines) were obtained from DFT E_b-F data for M_{13} clusters, presuming that $x_2 = 3.5$ Å (eq 2), and the corresponding $\Delta\Delta G^o-\phi$ plots (open symbols, dashed lines) were extracted from these by using eq 4. Clearly evident are the opposite signs of the $\Delta E_b-\phi$ and $\Delta\Delta G^o-\phi$ plots, the ϕ-dependent displacement between them necessarily being -1 eV/V (since here $z = -1$). (Further discussion of the relationships between potential/field-dependent binding energies defined with respect to neutral and charged bulk-phase reference states can be found in ref 14c.)

Combining eqs 1−4 leads simply to

$$\mu_S = ex_2(z - \gamma) \tag{5}$$

To the extent that the assumption of a linear potential drop across the inner layer is roughly valid, eq 5 furnishes a straightforward link between the field-dependent binding energetics addressed by DFT and the potential-dependent adsorption energies observed for electrochemical systems, the latter being expressed in terms of the electrosorption valency γ. Note that as the surface bond polarity (i.e., $|\mu_S|$) decreases, γ will approach z, reflecting a greater degree of "transfer" of the ionic charge ze to the metal upon ionic adsorption. For uncharged electrochemical adsorbates (i.e., when $z = 0$), then

$$\mu_S = -ex_2\gamma \tag{5a}$$

the proportionality constant $-ex_2$ merely reflecting the difference between the interfacial field and potential scales embodied in μ_S (eq 1) and γ (eq 3). In general, both μ_S and γ can depend on the applied interfacial field/potential as well as the adsorbate coverage. [This effect is evident in the perceptible nonlinearities in the E_b-F and $\Delta G^o-\phi$ plots for Hg(111)−I shown in Figure 1.] Consequently, then, strictly speaking the μ_S and γ values in eq 2 refer to a given interfacial field and the equivalent surface potential.

Similar relationships to eq 5 have been derived and utilized earlier, but from purely electrochemical thermodynamic considerations. Sass, Parsons, and co-workers[22a] obtained an expression for the surface−adsorbate dipole moment μ_S, which from their eqs 13 and 20 can be written (in conventional electrostatic units, esu) as

$$\mu_S/\epsilon_i = (z - \gamma)e(4\pi C_H)^{-1} \tag{6}$$

where ϵ_i is the inner-layer dielectric constant sensed by the dipolar adsorbate and C_H is the Helmholtz (or inner-layer) capacitance for a fixed adsorbate coverage. Since the latter term can be expressed as

$$C_H = \epsilon_i/4\pi x_2 \tag{6a}$$

combining eqs 6 and 6a leads to eq 5. Schmickler defined the electrode−adsorbate dipole moment to be[5,23]

$$\mu_S' = (4\pi)^{-1}(\partial\phi/\partial n)_{\sigma_{dif}} \tag{7}$$

where the partial differential refers to constant diffuse-layer charge σ_{dif}. In the case where $\sigma_{dif} = 0$, the net charge residing on the metal surface and adsorbate is zero. This definition therefore corresponds formally to the usual dipole-moment expression for adsorption of uncharged species at metal−UHV interfaces:[20,22,24]

$$\mu_S = (\epsilon_i/4\pi)(d\Phi/e\ dn) \tag{8}$$

where Φ is the metal work function and ϵ_i is usually taken as

unity. Setting $\epsilon_i = 1$ also in the presence of coadsorbed solvent, as in eq 7, is therefore tantamount to including solvent screening effects on the dipole-induced surface potential *formally* in the μ_S value itself, so that eq7 defines instead a "reduced" dipole moment given by

$$\mu_S' = \mu_S/\epsilon_i \tag{9}$$

which along with eq 6 leads to

$$\mu_S' = e(z - \gamma)(4\pi C_H)^{-1} \tag{10}$$

Parsons,[22b] Schmickler,[5,23] and Lipkowski and co-workers[25,26] have utilized eq 10 along with experimental values of γ and C_H to estimate reduced dipole moments for halides and other adsorbates at metal−aqueous interfaces. A virtue of evaluating μ_S' from eq 10 rather than μ_S from eq 5 is that the former contains only the experimental inner-layer capacitance C_H ($=\epsilon_i/4\pi x_2$) in addition to γ, so that the resulting μ_S' values are derived purely from measured quantities. On the other hand, while the extraction of μ_S from γ values via eq 5 requires estimating the inner-layer thickness x_2, the resulting dipole moments provide a measure of the "true" degree of metal−adsorbate charge polarization. Moreover, μ_S, and not μ_S', determines the field/potential dependence of the adsorption energy via eqs 1 and 5.

In any case the relation between μ_S' and μ_S (eq 9) is straightforward, so that the two quantities are readily interchangeable. It is worth emphasizing that the numerical values of μ_S' are markedly (often ≥10-fold) smaller than μ_S (vide infra), resulting from the dielectric screening embodied in the ϵ_i term which is contained within the inner-layer capacitance C_H in eq 10. The DFT calculations reported below refer to μ_S values for halogen adsorption both in the absence and presence of solvent dielectric, prompting comparison with dipole moments extracted from experimental γ data by using eq 5 rather than eq 10.

DFT Estimates of Surface Dipole Moments: Cluster Geometry Dependence. Before presenting the finite-cluster DFT results in comparison with electrochemical data, it is important to consider how the effective μ_S values extracted from DFT, μ_S(DFT), depend on the metal cluster size and shape. While the finite-cluster model can provide an acceptable description of an isolated surface−adsorbate bond, the calculated binding energies are known to be sensitive to the cluster size,[7a] and qualitatively similar effects might be expected for the surface dipole. A practical constraint on the cluster size, of course, is the time required for the DFT computations themselves. This factor limited us in our earlier ADF-DFT vibrational analyses for CO/NO on Pt-group metals to 25-atom or smaller clusters.[13] This restriction turns out to be less severe in the case of the gold, silver, and mercury clusters, of primary interest here. We have therefore undertaken an examination of the dependence of the μ_S(DFT) values for adsorbed Cl and I on the metal cluster size and shape. The Au(111)−Cl system is of particular interest because the availability of UHV work function−coverage data[27] enables experimental μ_S estimates to be obtained. (Unfortunately, such data are rare for halogen chemisorption.) While the adsorbate coverage calibration is somewhat uncertain,[28] the positive $\Delta\Phi - n$ slopes seen at low coverages yield from eq 8 (with $\epsilon_i = 1$) $-\mu_S \approx 1.0$ D. (Note that, by the usual convention, μ_S values are negative for electron-withdrawing adsorbates such as Cl.)

Table 1 lists values of $-\mu_S$(DFT) [in Debyes (D)] obtained for various Au_n−X and Hg_n−X clusters (X = Cl, I). Listed alongside (in parentheses) are corresponding "Hirshfeld" charges, $-q_H$, for the halogen atom; these values provide a rough estimate of the extent of metal−adsorbate charge donation.[18] The geometrical structure for each M_n cluster (far left-hand column) is denoted by the *a*/*b*/*c* values listed in parentheses, referring to the number of hexagonal close-packed atoms in the 1st/2nd/3rd layers. (The halogen adsorbate is bound in the central threefold-hollow site on the first layer.) The geometric variations were selected so to examine primarily the effects of varying the top-layer size and the cluster depth. Noticeable upon inspecting Table 1 is the greater sensitivity of the relative μ_S(DFT) values for Au_n−X versus Hg_n−X to the cluster size and geometry, along with the uniformly larger values for the latter. Both these observations can be reconciled with the anticipated greater Hg_n−X versus Au_n−X bond polarity. Interestingly, the q_H values are less sensitive to the cluster geometry, suggesting that the variations in μ_S(DFT) are due primarily to differences in the spatial distribution of the positive metal countercharge rather than the degree of metal−adsorbate charge donation. A similar insensitivity of q_H to the cluster size was noted for Ag(111)−Cl in ref 4a.

TABLE 1: Halogen Dipole Moments (D) and Hirshfeld Charges (e^-) from DFT for Various Au and Hg Cluster Geometries

	$-\mu_S{}^b$ ($-q_H$)^c			
cluster[a]	Au/Cl	Au/I	Hg/Cl	Hg/I
1 (1)	3.4 (0.22)	2.3 (0.12)	4.0 (0.31)	3.0 (0.23)
12 (6/6)	1.9 (0.14)	1.0 (0.05)	5.1 (0.45)	5.1 (0.35)
13 (6/7)	2.8 (0.24)	1.1 (0.06)	5.2 (0.47)	5.4 (0.37)
18 (12/6)	2.6 (0.23)	1.1 (0.06)	4.3 (0.50)	4.7 (0.42)
19 (6/6/7)	3.6 (0.26)	1.9 (0.11)	6.0 (0.46)	6.0 (0.36)
24 (12/12)	2.5 (0.29)	0.1 (0.05)	5.5 (0.49)	6.1 (0.43)
25 (12/6/7)	2.5 (0.28)	2.1 (0.08)	4.7 (0.50)	5.1 (0.43)
33 (21/12)	1.6 (0.26)	0.1 (0.11)	4.9 (0.49)	5.4 (0.43)
39 (27/12)	1.2 (0.25)	−0.2 (0.09)	4.4 (0.51)	5.0 (0.45)
40 (21/12/7)	1.1 (0.22)	0.6 (0.05)	6.3 (0.51)	6.8 (0.45)

[a] Total number of atoms in each Au and Hg cluster, followed by (in parentheses) the number of atoms in each fcc layer, denoted as first/second/third layer, with Cl or I adsorbed in a threefold-hollow site on the first layer. [b] Metal−adsorbate dipole moment (D) at zero external field from DFT for bond distances of: Au−Cl, 2.24 Å; Au−I, 2.53 Å; Hg−Cl, 2.52 Å; and Hg−Cl, 2.96 Å, where the distance (r_a) is the center-to-center perpendicular from the halogen to the top-layer metal plane. [The bond distances are the equilibrium values for the M_{13} clusters. Although slightly different (<0.05 Å) r_a values are obtained for the other cluster geometries, the μ_S and q_H values are essentially unaffected.] [c] Hirshfeld charge (e^-) on chlorine or iodine at zero external field from DFT (see text).

Examining further the Au_n−Cl data, some overall trends are evident. For the smaller clusters, $n \leq 25$, the $-\mu_S$(DFT) values lie mostly around 2.5 D (i.e., markedly larger than the above experimental estimate, $-\mu_S$(exp) ≈ 1.0 D). Expanding the top layer beyond the minimum number of Au atoms (6) required for hexagonal packing up to 12 atoms does not significantly bring μ_S(DFT) closer to μ_S(exp), and adding a third Au layer (as in the 6/6/7 cluster) even increases $-\mu_S$(DFT) further (Table 1). The latter observation, also seen (albeit more mildly) for the Hg_n−Cl systems, suggests that one reason that the $-\mu_S$(DFT) values are too high is the presence of Cl-induced charge polarization also on the cluster "backside", the additive dipolar effect being accentuated by the increased cluster depth.

Marked diminutions in $-\mu_S$(DFT) for Au_n−Cl, however, yielding values closer to experiment, are seen upon expanding the top layer further (beyond 12 atoms), as exemplified by the Au_{33}, Au_{39}, and Au_{40} clusters included in Table 1. Qualitatively similar, but milder, trends are evident for the corresponding Hg_n−Cl clusters. This effect suggests that a requirement for

TABLE 2: Metal−Halogen Dipole Moments (D) from DFT in Comparison with Experimental Estimates for Electrochemical Interfaces

		unsolvated interfaces								solvated interfaces				
		$-E_b$,[a] eV			$-q_H$[c]		$-\mu_S$(DFT)[d]		$(d\mu_S/dF)_{DFT}$[e]	$-q_H$(solv)[c]	$-\mu_s$(DFT,solv)[f]			
surface	adsorbate	M_{13}	M_{33}	r_a,[b] Å	M_{13}	M_{33}	M_{13}	M_{33}	M_{13}	M_{13}	M_{13}	$-\gamma$[g]	$-\mu_S$(exp)[h]	$-\mu_S'$(exp)[i]
Pt(111)	Cl	2.7		2.24	0.22		1.9		2.7	0.31	3.9	0.7−0.9[j]	∼**3**	
	Br	2.6		2.31	0.13		0.7		3.9	0.17	1.4			
	I	2.4		2.51	0.04		−0.1		5.5	0.04	−0.8			
Au(111)	Cl	2.4	1.7	2.24	0.24	0.26	2.8	1.3	2.5	0.34	5.5	0.4[k]	10	
	Br	2.2	1.5	2.34	0.16	0.19	2.0	0.8	3.6	0.21	3.7	0.6[k]	6.5	
	I	2.0	1.3	2.53	0.06	0.11	1.1	0.1	5.2	0.05	1.5	0.75[k]	4.0	
Ag(111)	Cl	3.0	2.3	2.14	0.28	0.35	3.1	1.3	1.9	0.40	6.3			
	Br	2.7	1.9	2.27	0.22	0.30	2.8	1.2	2.9	0.31	5.4	0.4−0.6[l]	∼8	
	I	2.3	1.5	2.48	0.14	0.24	2.3	1.4	4.4	0.20	4.2	0.6−0.8[l]	∼5	
Hg(111)	Cl	1.9	2.6	2.52	0.47	0.49	5.2	5.0	5.0	0.68	11.9	0.2[m]	13	1.15
	Br	1.6	2.4	2.69	0.43	0.46	5.1	5.2	6.7	0.64	11.9	0.34[m]	11	0.95
	I	1.1	2.0	2.96	0.37	0.43	5.4	5.4	9.4	0.59	12.0	0.45[m]	9	0.8

[a] Binding energy (eV) calculated from DFT for M_{13} or M_{33} cluster, as indicated, at zero field. [b] Metal−adsorbate bond distance (Å) threefold-hollow site from DFT for M_{13} clusters, taken as center-to-center perpendicularly from top-layer metal plane. [c] Effective (Hirshfeld) charge on adsorbate, from DFT. [d] Metal−adsorbate dipole moment (D) at zero external field from DFT. [e] Dipole moment−field dependence from DFT (in D/V Å^{-1}), at $F = 0$ for M_{13} clusters. [f] Metal−adsorbate dipole moment (D) at zero external field from DFT for M_{13} clusters embedded in a dielectric of 10, so to simulate solvation (see text). [g] Experimental values of electrosorption valency, taken sources cited for specific values (see text for details). [h] "Experimental" dipole moments, obtained from γ values by using eq 5, with $x_2 = 3.5$ Å (see text). [i] Experimental "reduced" dipole moment (for Hg/X only), obtained from γ values by using eq 5 with $C_H = 30$ μF cm^{-2} [so that $(4\pi C_H)^{-1} = 3 \times 10^{-9}$ cm (cf. refs 5, 23b)]. [j] Reference 31. [k] Reference 25c. [l] Reference 33. [m] Reference 21b.

mimicking the surface-dipolar properties of metal−electronegative adsorbate bonds with finite-cluster models is to include sufficient top-layer metal atoms so to enable the appropriate adsorbate-induced charge polarization to occur *along* the surface atomic plane. Without these additional top-layer atoms, it would appear that the electronegative adsorbate polarizes instead the second- and/or third-layer ("backside") metal atoms, producing dipolar components extending well beyond the M−X bond itself, and thereby yielding artificially large μ_S(DFT) values. (A related point is made on the basis of DFT calculations in ref 4b.) Roughly comparable cluster-geometry trends are evident for the less polar Au_n−I systems, although the variations in μ_S are accompanied by significant changes in q_H (Table 1). However, the low polarity of the Au_n−I compared to Au_n−Cl bonds is reflected by the generally small $-q_H$ values, ≤0.1, in addition to smaller $-\mu_S$ values. The markedly greater ionicity of the Hg_n−I bonds is signaled by the larger values of $-q_H$ as well as $-\mu_S$.

To some extent, these ambiguities can be avoided by undertaking DFT calculations based on periodic-slab, rather than finite-cluster, surface models. We have recently initiated calculations of metal−adsorbate dipole parameters (along with other bonding parameters) by using the former approach.[29] Briefly, μ_S values closer to experiment are obtained for chlorine adsorption on Pt-group and coinage metals than using the present finite-cluster approach. More generally, however, the agreement remains only semiquantitative; we are presently undertaking further studies along these lines.

Regardless of such details, the present finite-cluster approach is deemed sufficient for the largely illustrative purposes here. In the following section we have selected the M_{33} (21/12) cluster geometry for examining the sensitivity of μ_S(DFT) to the adsorbate and metal: very similar trends are also evident for larger clusters. We also include corresponding data for M_{13} (6/7) clusters. While the latter geometry would appear to overestimate μ_S(DFT), at least for Au(111), use of the smaller M_{13} cluster facilitates the DFT calculations, especially on the 5d Pt-group metals, and thereby has been utilized extensively by us for more computer-intensive DFT studies of adsorbate vibrational properties.[13] Moreover, the larger $-\mu_S$ values obtained by DFT for the dielectrically solvated clusters (vide infra) turn out to be relatively insensitive to the cluster geometry.

Comparison of Dipole Moments from DFT with Experimental Electrochemical Parameters. Contained in Table 2 are static dipole moments, μ_S(DFT), obtained by means of DFT for hollow-site binding of Cl, Br, and I atoms to unsolvated (111) surfaces, as modeled by M_{13} clusters of Pt, Au, Ag, and Hg, together with M_{33} clusters of the last three metals, in zero external field, $F = 0$. (Related DFT calculations have recently been presented for halogens on Pt, Hg, and Ag clusters.[4a]) Given that the $-\mu_S$ values usually depend significantly on field (cf. Figure 1), listed alongside are $(d\mu_S/dF)$ values extracted (at $F = 0$) from DFT for the 13-atom clusters. [At least for mercury, closely similar $(d\mu_S/dF)$ values were obtained with the M_{13} and M_{33} clusters.] Also included in Table 2 are the surface−adsorbate binding energies, E_b (eV), and the bond lengths, r_a (Å) (taken as the center-to-center perpendicular distance from the top-layer metal plane to the halogen atom), along with the Hirshfeld adsorbate charges,[18] q_H (e^-), all at $F = 0$. (For simplicity, r_a values are listed for only the M_{13} clusters.) As noted above, the M_{13}(6/7) cluster model clearly overestimates $-\mu_S$ for low-coverage M(111)−halogen systems. However, we have included these μ_S(DFT) values in Table 2 along with the more "realistic" M_{33} data; the former provide rough "upper-bound" estimates. Only M_{13} values are included for Pt(111), since DFT calculations for the larger clusters (including M_{33}) failed to converge. An experimental estimate of μ_S for the Pt(111)−Cl system, as for Au(111)−Cl, can be extracted from work-function data.[30] Surprisingly, small Φ decreases are observed at very low Cl dosages on Pt(111) prior to the sharp $\Delta\Phi-n$ increases expected for an electronegative adsorbate.[30] From the latter $\Delta\Phi-n$ slope, we deduce from eq 8 that $-\mu_S \sim 0.3$ D, again markedly smaller than the μ_S(DFT) estimate for the Pt_{13}−Cl cluster (Table 2).

In addition to the various μ_S(DFT) estimates, referring to adsorption on bare (i.e., unsolvated) clusters, corresponding values, labeled μ_S(DFT,solv), are included in Table 2 for M_{13} clusters imbedded in a "dielectric solvent" with $\epsilon_i = 10$. This

choice of ϵ_i is suggested by the typical values extracted from double-layer capacitance data.[5] In any case, the μ_S(DFT,solv) values are insensitive to ϵ_i (within ca. 20%) for $\epsilon_i > 5$. In addition, the dipole moments were found to be markedly less sensitive to the cluster geometry, μ_S(DFT,solv) values typically within 20% being obtained for the M_{13} and M_{33} clusters. Consequently, the μ_S(DFT,solv) values for only the former are listed in Table 2 for simplicity. Interestingly, the $-\mu_S$(DFT,solv) values are seen to be markedly (typically 2−5-fold) larger than the corresponding $-\mu_S$(DFT) values obtained for the M_{13} and M_{33} clusters. The notion that the solvation-induced dipole-moment enhancements reflect increased M−X bond polarity is supported by the larger negative Hirshfeld charges, $-q_H$(solv), obtained for the solvated clusters, which are also listed in Table 2. These enhancements in the bond polarity clearly reflect the stabilizing influence of the solvent dielectric. A qualitatively similar polarization effect was also reported in an early quantum-chemical study for Hg(111)−X, brought about by coadsorbing a single water molecule.[31]

It is of particular interest to examine the metal- and halogen-dependent trends in μ_S(DFT) and μ_S(DFT,solv) in comparison with experimental electrochemical values, extracted from eq 5, as another means of ascertaining the role of double-layer solvation in influencing the latter. To this end, Table 2 lists electrosorption valencies taken from thermodynamic analyses of halide adsorption on Pt(111),[32] Au(111),[25,26] Ag(111),[33] and Hg electrodes[21b] in aqueous solution. Where feasible, these γ values were selected to refer to low adsorbate coverages: due to the strong adsorption on Au(111) and Ag(111), data at more negative potentials were chosen. On Pt(111), however, hydrogen chemisorption obliged the use of γ estimates at slightly higher potentials (0−0.2 V vs SCE).[32] The "experimental" dipole moments, μ_S(exp), given alongside, were obtained from these γ values by using eq 5 and taking the inner-layer thickness, x_2, to be 3.5 Å. (While only approximate,[21] this last assumption is acceptable for the present rough comparative purposes.) It is worth mentioning that comparable μ_S(exp) values to those given in Table 2, referring to aqueous solution, can be obtained from data on mercury also in nonaqueous solvents, since the higher $-\gamma$ values obtained in the latter media can be correlated with the larger inner-layer thicknesses, x_2, evident from capacitance data.[21c]

Comparing the μ_S(DFT), μ_S(DFT,solv), and μ_S(exp) values in Table 2 is very instructive. Significantly, the corresponding μ_S(DFT,solv) and μ_S(exp) values for a given metal and adsorbate are similar, being within 20−30% except for the Ag(111)−X systems. Both these quantities, referring to solvated interfaces, are therefore markedly (≥2−3-fold) larger than the $-\mu_S$(DFT) values for the unsolvated surfaces. These differences therefore clearly reflect the stabilization of adsorbate negative charge by the surrounding inner-layer solvent, enhancing the bond ionicity. The marked variations in μ_S(exp) seen for a given adsorbate on the different metals correlate with the relative μ_S(DFT) and μ_S(DFT,solv) values, in the order Pt < Au < Ag < Hg. The same metal-dependent trend is also seen for the $-q_H$ and $-q_H$(solv) values, supporting its origin in variations of the bond ionicity. This sequence can readily be accounted for by differences in metal electron affinity or surface work function (cf. ref 4a). The dependence of μ_S(DFT) on the halogen at a given surface is also instructive (Table 2). While the bond polarity, as reflected roughly in $-q_H$, generally diminishes in the sequence Cl > Br > I, as might be expected, this halogen sensitivity is most marked for Au(111)−I and especially Pt(111)−I, where μ_S(DFT) ≈ 0 and q_H ≈ 0; i.e., the metal−iodine bond is essentially nonpolar. Interestingly, the $-\mu_S$(DFT,solv) and $-q_H$(solv) values for the Pt_{13}−I and Au_{13}−I systems are similarly small, indicating that the essentially covalent nature of these bonds is affected little by interfacial solvation. In contrast, the more polar Ag_{13}−I and especially Hg_{13}−I systems exhibit significant increases in both $-\mu_S$(DFT) and $-q_H$ upon solvation, in concert with the behavior of other metal−halogen cases, again reflecting the ability of the dielectric to enhance the bond ionicity.

In affording dielectric stabilization, the solvent also screens substantially the dipolar potential established by the polar metal−adsorbate bond. As noted above, such screening can be formally described in terms of a "reduced" dipole moment μ_S' defined by eq 10. For comparison, μ_S'(exp) values are also given for halides on mercury in Table 2, obtained from the γ values by using eq 10, with $C_H = 30\ \mu F\ cm^{-2}$.[34] (This "experimental" C_H value was utilized by Schmickler in his dipole-moment analysis.[5,23]) The μ_S'(exp) values are seen to be markedly (11.5-fold) smaller than the corresponding μ_S(exp) values, simply reflecting the effective ϵ_i value (11.5) obtained from eq 6a with $x_2 = 3.5$ Å.[32] Bearing in mind that for solvent-free interfaces, $\mu_S = \mu_S'$ (since then $\epsilon_i = 1$), the ca. 2-fold increase in μ_S brought about by interfacial solvation for the Hg−X systems is more than offset by the dielectric screening of the dipolar potential drop, yielding μ_S' decreases upon solvation. These solvation effects on μ_S' are generally expected to be compensating; this accounts for the relatively small changes in the $\Delta\phi-\Delta n$ slopes induced by the presence of interfacial solvent observed for some systems.[22,23] It should be borne in mind, however, that the "true" surface−adsorbate dipole moment in terms of fundamental electrostatics is μ_S, not μ_S'.

Finally, the DFT results can provide insight into the dependence of the bond polarity on the electrode potential. The positive $(d\mu_S/dF)_{DFT}$ values listed in Table 2 indicate that, as might be expected, the metal−halogen bonds become less polar as the interfacial field becomes less negative/more positive. The uniform increase of $(d\mu_S/dF)$ seen in the sequence Cl < Br < I is anticipated from the corresponding order of adsorbate polarizabilities. Given that changes in electrode potential of ca. 2 V are often accessible to experiment, and $\Delta\phi = 2$ V roughly corresponds to $\Delta F \sim 0.7\ V\ Å^{-1}$, substantial changes in μ_S may often be expected under these conditions. For example, over this interfacial-field range with $F = 0$ as the midpoint, μ_S(DFT) changes from ca −2 to 2 D for Pt(111)/I and from −9 to −3 D for Hg(111)/I. Unfortunately, the interpretation of potential-dependent γ values in this fashion is often complicated by the effects of varying adsorbate coverage and inner-layer dielectric properties. Nevertheless, the experimental $-(d\gamma/dE)$ value for the Hg/I system at low coverages, $0.14\ V^{-1}$,[21b] leads to $(d\mu_S/dE) \sim 2.5\ D\ V^{-1}$. The resulting experimental $(d\mu_S/dF)$ estimate, ca. 8 D/V $Å^{-1}$, is comparable to the corresponding DFT value given in Table 2.

Concluding Remarks

Overall, the DFT calculations furnish trends in the surface−adsorbate bond polarity for these archetypical metal electrode−halogen systems which are not only roughly consistent with thermodynamic electrochemical measurements for halide adsorption but also provide insight into the important influences exerted by double-layer solvation. The reasonable agreement seen between the adsorbate values of μ_S(DFT,solv) and μ_S(exp), as well as the variations induced by altering the metal and/or the halogen, are also encouraging, despite the admittedly crude nature of the present dielectric-solvation model. Given eqs 1−4,

this agreement suggests a practical usefulness of DFT calculations in predicting field-/potential-dependent binding energies. The findings also give us some confidence in applying these and related DFT-based models to describe potential-dependent metal−adsorbate vibrational frequencies in terms of bond length-dependent (i.e., dynamical) dipole moments. This issue is discussed in detail elsewhere.[14]

More generally, the above analysis connecting field-dependent *halogen* binding and potential-dependent *halide* adsorption emphasizes the link inherent between these properties, accessed experimentally in metal−UHV and electrochemical systems, respectively. Given the limitations in the finite-cluster DFT approach for estimating bond polarity, as noted above it would be worthwhile to undertake further periodic slab calculations along these lines, which we are presently pursuing. Including discrete coadsorbed solvent and ionic/electronic charge in the DFT surface model would be of particular interest as a means of treating double-layer solvation in a more realistic fashion than the "fixed dielectric constant" solvent formalism employed here. Overall, then, such DFT-based model calculations clearly have the potential to provide broad-based quantum-chemical insight into the factors controlling adsorbate bonding at electrochemical and other electrified interfaces.

Acknowledgment. We are indebted to Prof. Jens Nørskov for pointing out to us the significance of eq 1. We are also grateful to Prof. Roger Parsons for helpful comments regarding the definition of dipole moments for electrochemical adsorbates. This work is supported by the Petroleum Research Fund and the National Science Foundation (Analytical and Surface Chemistry Program).

References and Notes

(1) For example, see: (a) Delahay, P. *Double Layer and Electrode Kinetics*; Interscience: New York, 1965. (b) Grahame, D. C. *Chem. Rev.* **1947**, *41*, 441.

(2) (a) Barclay, D. C. *J. Electroanal. Chem.* **1970**, *28*, 443. (b) Barclay, D. C.; Caja, J. *Croat. Chim. Acta* **1971**, *43*, 221.

(3) (a) Anson, F. C. *Acc. Chem. Res.* **1975**, *8*, 401. (b) Parsons, R. *Chem. Rev.* **1990**, *90*, 813.

(4) For earlier quantum-chemical studies related to the present work, see: (a) Koper, M. T. M.; van Santen, R. A. *Surf. Sci*. **1999**, *422*, 118. (b) Ignaczak, A.; Gomes, J. A. N. F. *J. Electroanal. Chem.* **1997**, *420*, 71. (c) Blanco, M.; Rubio, J.; Illas, C. F. F. *J. Electroanal. Chem.* **1989**, *261*, 39. (d) Illas, F.; Rubio, J.; Ricart, J. M.; Garrido, J. A. *J. Electroanal, Chem.* **1986,** *200*, 47.

(5) Schmickler, W. in *Structure of Electrified Interfaces*; Lipkowski, J., Ross, P. N., Eds.; VCH Publishers: New York, 1993; Chapter 6.

(6) For example: (a) Weaver, M. J.; Gao, X. *Annu. Rev. Phys. Chem*. **1993**, *44*, 459. (b) Weaver, M. J. *J. Phys. Chem.* **1996,** *100*, 13079.

(7) For example: (a) van Santen, R. A.; Neurock, M. *Catal Rev.-Sci. Eng*. **1995**, *37*, 557. (b) Minot, C.; Markovits, A. *J. Mol. Struct*. **1998**, *424*, 119. (c) Hammer, B.; Nørskov, J. K. *Adv. Catal*. **2000**, *45*, 71.

(8) (a) Bagus, P. S.; Pacchioni, G. *Electrochim. Acta* **1991**, *36*, 1669. (b) Pacchioni, G.; Bagus, P. S.; Philpott, M. R.; Nelin, C. J. *Int. J. Quantum Chem*. **1990**, *28*, 675.

(9) Head-Gordon, M.; Tully, J. C. *Chem. Phys*. **1993**, *175*, 37.

(10) (a) Illas, F.; Mele, F.; Curulla, D.; Clotet, A.; Ricart, J. M. *J. Electrochim. Acta* **1998**, *44*, 1213. (b) Curulla, D.; Clotet, A.; Ricart, J. M.; Illas, F. *Electrochim. Acta* **1999**, *45*, 639. (c) Garcia-Hernandez, M.; Curulla, D.; Clotet, A.; Illas, F. *J. Chem. Phys*. **2000**, *113*, 364.

(11) Liao, M. S.; Zhang, Q.-E. *J. Chem. Soc. Faraday Trans*. **1998**, *94*, 1301.

(12) (a) Koper, M. T. M.; van Santen, R. A. *J. Electroanal. Chem*. **1999**, *472*, 126. (b) Koper, M. T. M.; van Santen, R. A. *J. Electroanal. Chem*. **1999**, *476*, 64.

(13) (a) Koper, M. T. M.; van Santen, R. A.; Wasileski, S. A.; Weaver, M. J. *J. Chem. Phys*. **2000**, *113*, 4392. (b) Wasileski, S. A.; Koper, M. T. M.; Weaver, M. J. *J. Phys. Chem. B* **2001**, *105*, 3518. (c) Wasileski, S. A.; Weaver, M. J.; Koper, M. T. M. *J. Electroanal. Chem*. **2001**, *500*, 344.

(14) (a) Wasileski, S. A.; Koper, M. T. M.; Weaver, M. J. *J. Chem. Phys.* **2001**, *115*, 8193. (b) Wasileski, S. A.; Koper, M. T. M.; Weaver, M. J. *J. Am. Chem. Soc.* **2002**, *124*, 2796. (c) Wasileski, S. A.; Weaver, M. J. *J. Electroanal. Chem.*, in press. (d) Wasileski, S. A.; Weaver, M. J. *Faraday Discuss.*, in press.

(15) For a review, see: Weaver, M. J.; Zou, S. Spectroscopy for Surface Science. In *Advances in Spectroscopy;* Clark, R. J. H., Hester, R. E., Eds.; Wiley: Chichester, 1998; Vol. 26, Chapter 5.

(16) (a) Amsterdam Density Functional Package, ADF 2000.03, Department of Theoretical Chemistry, Vrije Universiteit, Amsterdam, 2000. (b) Pyle, C. C.; Ziegler, T. *Theor. Chem. Acc.* **1999,** *101*, 396. (c) Baerends, E. J. Ellis, D. E.; Ros, R. *Chem. Phys.* **1973**, *2*, 41. (d) teVelde, G.; Baerends, E. J. *J. Comput. Phys.* **1992**, *99*, 84.

(17) (a) Vosko, S. H.; Wilk, L.; Nusair, M. *Can. J. Phys.* **1980**, *58*, 1200. (b) Becke, A. D. *Phys. Rev. A* **1988**, *39*, 3098. (c) Lee, C.; Yang, W.; Parr, P. G. *Phys. Rev. B* **1988**, *37*, 785.

(18) (a) Hirshfeld, F. L. *Theor. Chim. Acta* **1977**, *44*, 129. (b) See also: Wiberg, K. B.; Rablen, P. R. *J. Comput. Chem.* **1993**, *14*, 1504.

(19) (a) Mortensen, J. J.; Hammer, B.; Nørskov, J. K. *Surf. Sci*. **1998**, *414*, 315. (b) Nørskov, J. K.; Holloway, S.; Lang, N. D. *Surf. Sci.* **1984**, *137*, 65.

(20) For example: (a) Macdonald, J. R.; Barlow, C. A., Jr. *J. Chem. Phys*. **1963**, *39*, 412. (b) Hölzl, J.; Schulte, F. K. In *Springer Tracts in Modern Physics*; Hohler, G., Niekisch, E. A., Eds.; Springer: Berlin, 1979; Vol. 85, p 1. (c) Wandelt, K. In *Physics and Chemistry of Alkali Metal Adsorption*; Bonzel, H. P., Bradshaw, A. M., Ertl, G., Eds.; Elsevier: Amsterdam, 1989; p 25.

(21) (a) Schultze, J. W.; Vetter, K. J. *J. Electroanal. Chem*. **1973**, *44*, 63. (b) Schultze, J. W.; Koppitz, F. D. *Electrochim. Acta* **1976**, *21*, 327. (c) Schultze, J. W.; Koppitz, F. D. *Electrochim. Acta* **1976**, *21*, 337.

(22) (a) Bange, K.; Strachler, B.; Sass, J. K.; Parsons, R. *J. Electroanal. Chem*. **1987**, *229*, 87. (b) Parsons, R. *Bull. Electrochem.* **1990**, *6*, 566.

(23) (a) Schmickler, W. *J. Electroanal. Chem*. **1988**, *249*, 25. (b) Schmickler, W. *Ber. Bunsen-Ges. Phys. Chem*. **1988**, *92*, 1203.

(24) Expressions equivalent to eq 8, but with the coefficient 2π replacing 4π, are sometimes written: these correspond to the dipole moment defined in terms of an adsorbate charge−image charge, rather than charge−metal surface separation.[20c]

(25) (a) Shi, Z.; Lipkowski, J. *J. Electroanal Chem*. **1996**, *403*, 225. (b) Shi, Z.; Lipkowski, J.; Mirwald, S.; Pettinger, B. *J. Chem. Soc. Far. Trans*. **1996**, *92*, 3737. (c) Chen, A.; Shi, Z.; Bizzoto, D.; Lipkowski, J.; Pettinger, B.; Bilger, C. *J. Electroanal. Chem*. **1999**, *467*, 342. (d) Chen, A.; Lipkowski, J. *J. Phys. Chem. B* **1999**, *103*, 682.

(26) Lipkowski, J.; Shi, Z.; Chen, A.; Pettinger, B.; Bilger, C. *Electrochim. Acta* **1998**, *43*, 2875.

(27) Kastanas, G. N.; Koel, B. E. *Appl. Surf. Sci.* **1993**, *64*, 235.

(28) We assume here that the ($\sqrt{3}$ x $\sqrt{3}$) structure observed by LEED for Au(111)/Cl in ref 27 corresponds to a fractional coverage $\theta = {}^1/_3$.

(29) The periodic-slab calculations employed the DACAPO code (Center for Atomic-Scale Materials Physics, Technical University of Denmark).

(30) Villegas, I.; Weaver, M. J. *J. Phys. Chem*. **1996**, *100*, 19502.

(31) Kuznetsov, A.; Reinhold, J.; Lorenz, W. *J. Electroanal. Chem.* **1984**, *104*, 167.

(32) Li, N.; Lipkowski, J. *J. Electroanal. Chem*. **2000**, *491*, 95.

(33) Foresti, M. L.; Innocenti, M.; Forni, F.; Guidelli, R. *Langmuir* **1999**, *14*, 7008.

(34) Unlike mercury, a complication in applying this analysis for the halides on Au(111) (and other solid metals) is that the C_H values are strongly dependent on the electrode potential as well as on the identity and coverage of the halide.[25c,26] While this behavior reflects alterations in the inner-layer dielectric properties, the resulting variations in μ_S' [25c,26] do not necessarily correspond to changes in the *charge* distribution of the surface−adsorbate bond that is sensed by γ and μ_S. Values of μ_S' are therefore given only for mercury in Table 2.